Struct Chem (2017) 28:123–132
DOI 10.1007/s11224-016-0843-5

ORIGINAL RESEARCH

Mackay clusters and beyond in icosahedral quasicrystals seen from 6D space

Abdullah Sirindil[1] · **Marianne Quiquandon**[1] · **Denis Gratias**[1]

Received: 18 July 2016 / Accepted: 30 August 2016 / Published online: 22 September 2016

Abstract It is a great pleasure and honour for us to participate to the celebration of the 90th birthday of Alan Mackay, one of the most inspired crystallographers of our time who has been the authentic predecessor of the quasicrystal discovery. We discuss here several ways to construct Mackay-type atomic clusters and others for describing quasicrystalline structures from the standard 6D framework. We show that they are several simple solutions for both the 6D natural cluster and the original Mackay derivation that are consistent with special points of the basic icosahedral 6D lattice and the actually determined clusters in usual cubic 1/1 approximants of the icosahedral phases. This technique works as well for describing the two first shells of the so-called Bergman clusters but the situation is far more complicated for the so-called Tsai cluster that cannot be directly obtained from the icosahedral cut and projection of the simple 6D lattice special points without significantly large differences in the radii of the various orbits with respect to their actual positions in the YbCd icosahedral-type alloys. This shows that the 6D approach using special points as locations of the mean atomic surfaces—although very efficient for constructing initial simple models of the icosahedral phases—requires subsequent refinement techniques, especially in the actual locations and sizes of the various atomic orbits of the implied clusters, for leading to final acceptable structural models.

✉ Denis Gratias
denis.gratias@chimie-paristech.fr

[1] IRCP Chimie-ParisTech, PSL Research University, Paris, France

Keywords Quasicrystals · Crystalline structures · Hyperspace crystallography · Mackay cluster · Bergman cluster · Tsai cluster

Introduction

On 8 April 1982, at the National Bureau of Standards (Gaithersburg Maryland USA), Dan Shechtman [1] observed an impossible electron diffraction pattern in rapidly solidified alloy close to the composition Al_6Mn with well-defined typical crystalline Bragg peaks but distributed on regular decagons! In his notebook, he wrote "ten-fold???" in front of the micrograph reference number.

It turned out that most of the basic questions posed by this apparently paradoxical and revolutionary observation had already been almost completely answered by Alan L. Mackay in two previous papers.

The first paper [2] *De Nive Quiquangula: On the pentagonal snowflake* was submitted to Kristallographyia on 4 April 1981 and published in the September–October issue. Alan L. Mackay explicitly demonstrated the possible relevance of the Penrose 2D tiling and its 3D equivalent (rhombic triacontahedron) in modern crystallography. Alan L. Mackay wrote in this first paper almost exactly 1 year before Shechtman's first observation of quasicrystals: "...it gives an example of a pattern of the type which might well be encountered but which might go unrecognized if unexpected ...".

The second paper [3] is the experimental demonstration that Penrose patterns diffract on an apparently discrete set of Bragg peaks—in fact, a dense enumerable set with almost all peaks having weak intensities for being observable—by irradiating a photograph of a Penrose pattern by a LASER beam.

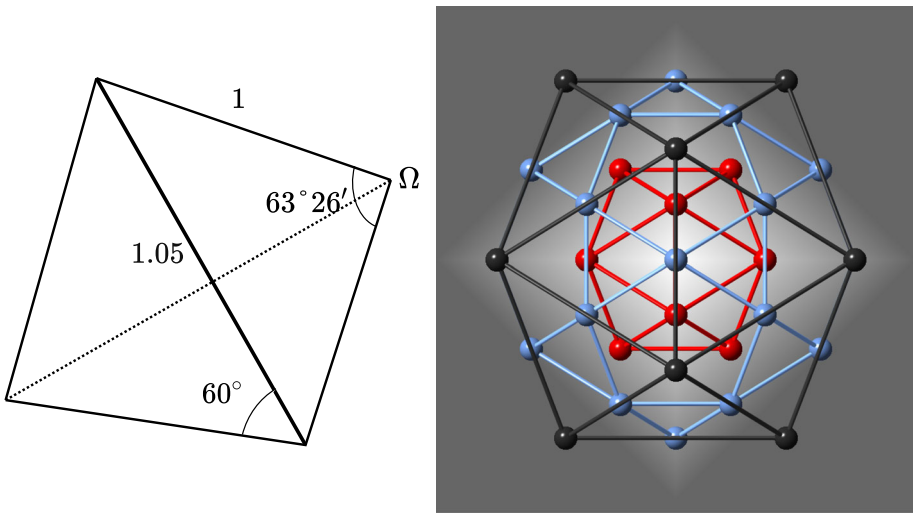

Fig. 1 Ideal Mackay cluster is the stacking of the two first shells of an almost perfect tetrahedron, drawn on the *left*, defined by a triangular facet and the center of a regular icosahedron. This cluster is made of 54 sites plus a center: a small inner icosahedron (12) and extra shell of an icosidodecahedron (30) with atoms on the middle of the edges of an external icosahedron (12) of radius twice larger than the inner one

The two papers contained the very basic ingredients for the understanding of Shechtman's paradoxical electron diffractions, but, unfortunately, he and his co-authors—and perhaps, much later, the members of the Nobel committee for Chemistry ...—were not aware of them. Beyond these two outstanding articles, Alan L. Mackay wrote another fundamental piece [4] of crystallography in 1962 where he proposed a new possible icosahedral atom packing for small aggregates. The basic ingredient is the elementary tetrahedron defined by the center Ω and the three vertices $\{(0,0,0),(1,\tau,0),(\tau,0,1),(0,1,\tau)\}$ of one of the triangular faces of a regular icosahedron as shown in Fig. 1. This is an almost perfect regular tetrahedron with two very close lengths of edge in the ratio $2\sqrt{(3-\tau)/5} \approx 1.05146$ with one equilateral triangular facet and the three others with an angle $\cos\alpha = \tau/(2+\tau)$, i.e., $\alpha \approx 63°26'$.

Mackay' idea was to design a new type of packing around a center using this kind of tetrahedra. Hence, the first shell of the cluster is the icosahedron itself and the second shell with 42 atoms is an icosahedron twice larger plus an icosidodecahedron generating the new vertices at the mid-edges of the large icosahedron as shown in the right of Fig. 1. The construction process was thus iterated to any order n by adding icosahedra of radius n times larger that the initial ico and filling the triangular facets in an hexagonal 2D network like the (1, 1, 1) planes in a FCC metal.

In fact, only the icosahedral cluster made of the *two first atomic shells* has so far been experimentally identified in complex metallic alloys. It is made of (see Fig. 1):

- a center that is or not occupied by an atom;
- a first shell of a inner icosahedron of radius[1] $\sqrt{2+\tau}/2$;
- a second shell with a large icosahedron of radius $\sqrt{2+\tau}$ twice larger that the previous one;
- an icosidodecahedron of radius τ belonging to the second shell.

This specific cluster of 54 sites is actually called the *Mackay cluster*. It was proven early on [5–8] to be one of the basic atomic units in the structure of many icosahedral quasicrystals and their approximants.

By extension, we designate as *Mackay-type* clusters, atomic clusters that have a double icosahedron plus an icosidodecahedron not necessarily in the ideal ratio previously given. Finally, *pseudo-Mackay* clusters are clusters with an icosahedron plus a icosidodecahedron as second shell with no specific requirement concerning the first shell (see for instance [9]).

Our present purpose here is to discuss how the Mackay clusters and their derivatives are easily and nicely generated in the cut algorithm from periodic 6D description of the icosahedral phases. To achieve this goal, we shall first give a brief review of the cut and project method and the basic ND crystallography concepts used to describe quasicrystals. In the second part, we will review the various avatars of the Mackay clusters that are encountered in both icosahedral and approximant structures and discuss how they integrate into the general 6D scheme of using special points in the frame of the cut and project method. We will finally discuss shortly the other typical atomic clusters frequently encountered in the icosahedral phases.

N-dim crystallography

As initially demonstrated by de Bruijn [10, 11] for Penrose tilings, ideal quasicrytals can be described as 3-dim cuts of periodic objects in $N > 3$-dim space, $\mathbf{E}^N$, irrationally oriented with respect to the N-dim lattice Λ of the periodic

[1] This choice of length scale will be made clear latter in the text.

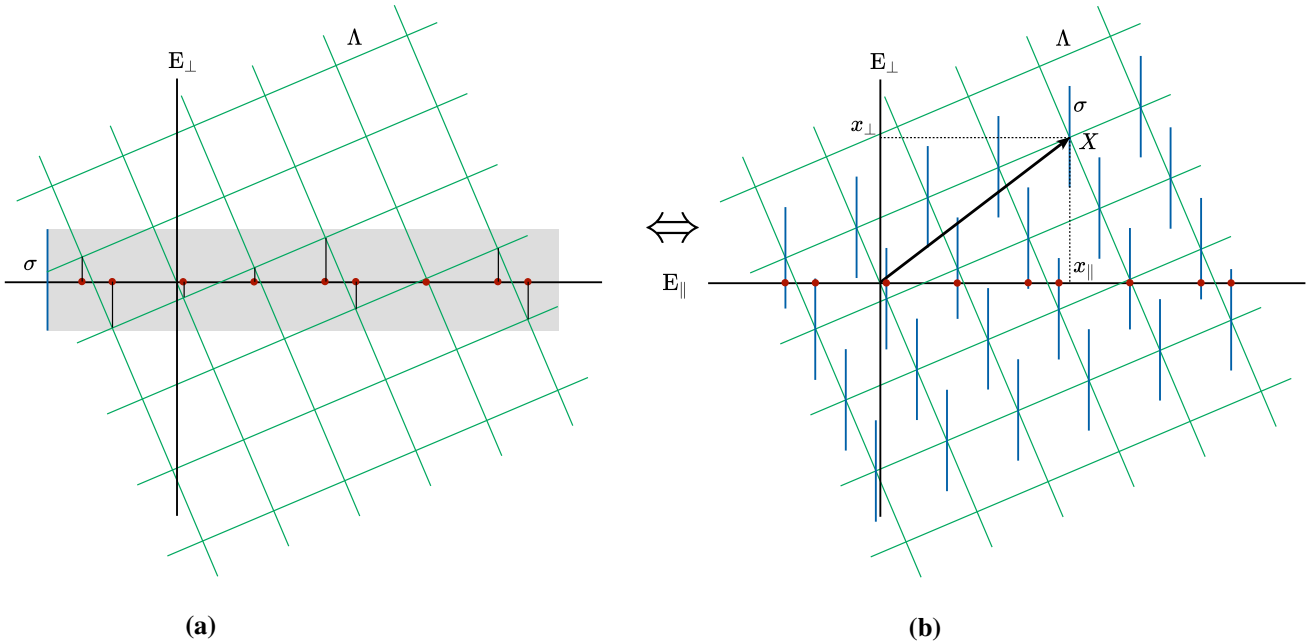

(a) **(b)**

Fig. 2 **a** The cut method corresponding to the Definition 3 is equivalent in copying the acceptance window σ at each lattice node as drawn in (**b**). This allows for a natural generalization of the notion of Wyckoff positions in $\mathbf{E}^N$: a quasiperiodic structure is defined by a set of positions X_i in the N-dim unit cell, each associated with a given specific acceptance window σ_i that we call *atomic surface* to conform to the superspace description (see for instance [15]) used for incommensurate structures

structure, sketched in Fig. 2 as independently proposed by Duneau and Katz [12], Elser [13] and Kalugin et al. [14]. This method, known as the cut method, is a direct and simple way of generating quasiperiodic tilings often called model sets $\mathscr{M}$. It uses the following ingredients:

- a N-dim space $\mathbf{E}^N$, here $\mathbb{R}^6$, having a pair of complementary subspaces: $\mathbf{E}_\parallel$, here $\mathbb{R}^3$, is the physical space containing the model set characterized by the projector $\hat{\pi}_\parallel$ and $\mathbf{E}_\perp$, here $\mathbb{R}^3$, the internal space characterized by the complementary projector $\hat{\pi}_\perp$, and such that:

$$\mathrm{E}^N = \mathbf{E}_\parallel \oplus \mathbf{E}_\perp \tag{1}$$

$$\forall X \in \mathrm{E}^N \quad X = x_\parallel + x_\perp, \quad x_\parallel = \hat{\pi}_\parallel X, \quad x_\perp = \hat{\pi}_\perp X \tag{2}$$

- a lattice $\Lambda \subset \mathbf{E}^N$; and
- one or several bounded windows or acceptance windows $\sigma \subset \mathbf{E}_\perp$ that define the so-called atomic surfaces in $\mathbf{E}_\perp$. The quasiperiodic set $\mathscr{M}$ is thus defined by:

$$\mathscr{M} = \{\hat{\pi}_\parallel \lambda,\ \lambda \in \Lambda \mid \hat{\pi}_\perp \lambda \in \sigma\} \tag{3}$$

Real quasicrystals are usually described with several acceptance windows σ_i associated with the various atomic species and their geometric environments; they play the same role as Wyckoff positions for standard crystals.

Atomic surfaces associated with atomic clusters

The first task to achieve is to find a systematic procedure that allows for the definition of the atomic surfaces (AS) associated with a given *atomic cluster* defined as a set of neighbor atoms that repeats with a high frequency in the structure such that *if* one *atom of the set is present in the structure then* all *atoms of the set are present: the same set of atoms occurs in the same configuration*.

Let σ_0 be the AS associated with the center of the cluster. Our main assumption is that the cluster is a set of positions $\hat{\pi}_\parallel t_j$ corresponding to the parallel projections of rational positions[2] t_j in Λ of $\mathbf{E}^N$. The way of defining the complete set of ASs generating the cluster in N-dim spaces is sketched in Fig. 3 and goes as follows.

- Copy σ_0 parallel to $\mathbf{E}_\parallel$ at the various locations $\hat{\pi}_\parallel t_j$ defining the cluster.
- Associate each translated σ_0 on the locations t_j displaced in $\mathbf{E}_\perp$ by $\hat{\pi}_\perp t_j$.
- Complete this AS around t_j with all its copies in the little group H of t_j.

[2] The key point in the present approach is that each atomic position in $\mathbf{E}_\parallel$ must unambiguously be considered as the parallel projection of one and only one position in $\mathbf{E}^N$.

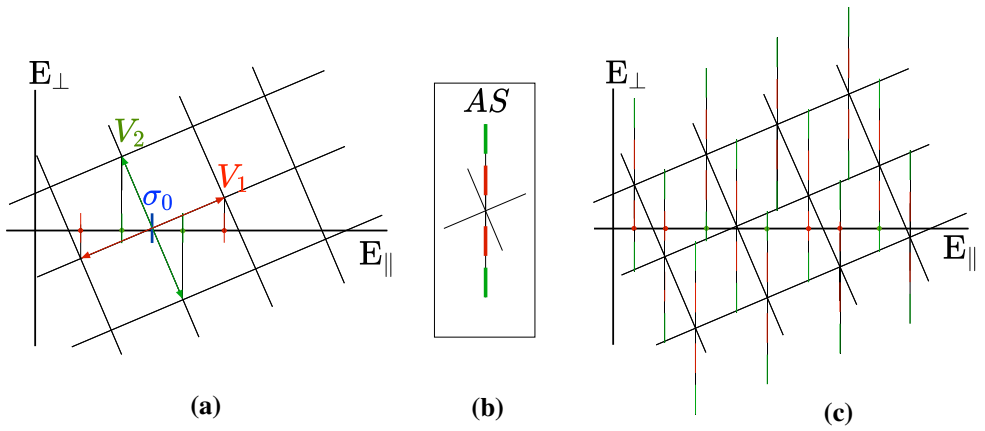

Fig. 3 A simple example of constructing the AS necessary to generate a specific cluster starting from the AS σ_0 (*blue*) generating the center of the cluster. **a** The *red–green* cluster is defined by two orbits, *red* and *green*, that are projections in $\mathbf{E}_\parallel$ of lattice points $t_1 = (n, m)$. We copy σ_0 along the horizontal line ($\mathbf{E}_\parallel$) at the level of the projections of the lattice nodes (*red*) and (*green*). **b** Copying these surfaces on all equivalent sites, we obtain the set of atomic surfaces that generates the red–green cluster. **c** General drawing of the full 2D model: any horizontal cut leads to a quasiperiodic sequence of red–green clusters (Color figure online)

Thus, an atomic cluster AC made of N orbits of atoms, each orbit j of M_j surrounding atoms characterized by translations $\hat{\pi}_\parallel t_j^k$ is defined by:

$$\mathrm{AC} = \cup_{j=1}^{N} \cup_{k=1}^{M_j} \hat{\pi}_\parallel t_j^k;$$

its corresponding generating global AS, say $\mathrm{AS_{AC}}$, is obtained by the union of all σ_0's located in $\mathbf{E}_\perp$ at $\hat{\pi}_\perp t_j^k$ sites in 6D:

$$\mathrm{AS_{AC}} = \cup_{j=1}^{N} \cup_{k=1}^{M_j} \sigma_0(\hat{\pi}_\perp t_j^k).$$

The AS attached to the position t_j is a copy of σ_0 displaced by $\hat{\pi}_\perp t_j$ completed by its copies in the little group H of order n_j, of t_j:

$$\mathrm{AS}_j = \cup_{k=1}^{n_j} \sigma_0\left(\hat{h}_k \hat{\pi}_\perp t_j\right); \quad \hat{h}_k \in H \tag{4}$$

This formula applies for any kind of atomic clusters whatever symmetry and/or dimension of the configurational space. The choice of σ_0 is crucial. The first criterion is to choose σ_0 as large as possible in order to have the highest frequency of clusters—that are supposed to be typical—in the structure. The second criterion is that most of the atoms of the clusters should belong to one cluster only. This requires that for any two σ_0, say k and k', of a given orbit of the cluster has no intersection:

$$\forall h_k, h_{k'} \in H \; k \neq k', \quad \sigma_0(\hat{h}_k \hat{\pi}_\perp t_j) \cap \sigma_0(\hat{h}_{k'} \hat{\pi}_\perp t_j) = \emptyset$$

The icosahedral phase is described in a 6D space that decomposes into the two usual 3D subspaces $\mathbf{E}_\parallel$ and $\mathbf{E}_\perp$. The real physical space $\mathbf{E}_\parallel$ is generated by the three vectors orthonormal vectors $\{|\alpha\rangle\}$, and $\mathbf{E}_\perp$ is generated by the three orthonormal vectors $\{|\bar{\alpha}\rangle\}$. The orthonormal basis of the 6 unit vectors $\{|1\rangle, \ldots, |6\rangle\}$ in 6D projects in $\mathbf{E}_\parallel$ and $\mathbf{E}_\perp$ according to the coordinates given in Table 1. Introducing $\mathscr{K} = 1/\sqrt{2(2+\tau)}$, we thus obtain the matrix $\widehat{\mathbf{R}}$ relating the reference frame $\{|1\rangle, \ldots, |6\rangle\}$ with $\{|\alpha\rangle, |\bar{\alpha}\rangle\}$:

$$\widehat{\mathbf{R}} = \mathscr{K} \begin{pmatrix} 1 & \tau & 0 & -1 & \tau & 0 \\ \tau & 0 & 1 & \tau & 0 & -1 \\ 0 & 1 & \tau & 0 & -1 & \tau \\ -\tau & 1 & 0 & \tau & 1 & 0 \\ 1 & 0 & -\tau & 1 & 0 & \tau \\ 0 & -\tau & 1 & 0 & \tau & 1 \end{pmatrix};$$

$$\times \begin{pmatrix} \alpha_x \\ \alpha_y \\ \alpha_z \\ \bar{\alpha}_x \\ \bar{\alpha}_y \\ \bar{\alpha}_z \end{pmatrix} = \widehat{\mathbf{R}} \begin{pmatrix} n_1 \\ n_2 \\ n_3 \\ n_4 \\ n_5 \\ n_6 \end{pmatrix}$$

Table 1 Coordinates of the projections of the 6 unit vectors $|i\rangle$, $\langle\alpha|i\rangle$ in $\mathbf{E}_\parallel$, and $\langle\bar{\alpha}|i\rangle$ in $\mathbf{E}_\perp$, for the icosahedral phases in 6D

$\langle\alpha\|i\rangle$	1	2	3	4	5	6
x	1	τ	0	-1	τ	0
y	τ	0	1	τ	0	-1
z	0	1	τ	0	-1	τ

$\langle\bar{\alpha}\|i\rangle$	1	2	3	4	5	6
x'	$-\tau$	1	0	τ	1	0
y'	1	0	$-\tau$	1	0	τ
z'	0	$-\tau$	1	0	τ	1

Table 2 Special positions and their little groups in the 6D unit-cell for the groups *Pm*35 (G_P) and *Fm*35 (G_F)

$[N, M] \times 4$	μ	X_6	G_P	G_F
[0, 0]	1	(0,0,0,0,0,0)	m35(120)	m35(120)
[2, 1]	12	(1,0,0,0,0,0)/2	$\bar{5}$m(20)	5m(10)
[4, 0]	30	(1,0,0,0,0,1)/2	mmm(8)	mmm(8)
[4, 4]	30	(1,1,0,0,0,0)/2	mmm(8)	mmm(8)
[6, 9]	20	(1,1,1,0,0,0)/2	$\bar{3}$m(12)	3m(6)
[6, 5]	60	(1,1,0,1,0,0)/2	$\bar{3}$m(12)	3m(6)
[6, 1]	60	(1,0,0,0,1,1)/2	$\bar{3}$m(12)	3m(6)
[6, −3]	20	(0,0,0,1,1,1)/2	$\bar{3}$m(12)	3m(6)
[8, 12]	30	(1,1,1,1,0,0)/2	mmm(8)	mmm(8)
[8, 8]	60	(1,1,0,1,1,0)/2	mmm(8)	mmm(8)
[8, 4]	60	(0,1,1,1,1,0) /2	mmm(8)	mmm(8)
[8, 0]	60	(0,0,1,1,1,1)/2	mmm(8)	mmm(8)
[8, −4]	30	(0,0,$\bar{1}$,1,1,1) /2	mmm(8)	mmm(8)
[10, 13]	60	(1,1,1,1,1,0)/2	$\bar{5}$m(20)	5m(10)
[10, 5]	12	(0,1,1,1,1,$\bar{1}$)/2	$\bar{5}$m(20)	5m(10)
[10, 5]	60	(1,0,1,1,1,1)/2	$\bar{5}$m(20)	5m(10)
[10, −3]	60	(0,$\bar{1}$,1,1,1,1)/2	$\bar{5}$m(20)	5m(10)
[12, 16]	12	(1,1,1,1,1,$\bar{1}$)/2	m35(120)	m35(120)
[12, 12]	20	(1,1,1,1,1,1)/2	m35(120)	m35(120)
[12, 0]	20	($\bar{1}$,1,1,1,1,1)/2	m35(120)	m35(120)
[12, −4]	12	($\bar{1}$,1,1,1,1,$\bar{1}$)/2	m35(120)	m35(120)

Under these notations, the main special positions of the groups *Pm*35 and *Fm*35 are listed in Table 2.

The simplest possible atomic clusters are those that are generated from the highest symmetry special positions V_j in $\mathbf{E}^6$. In the present case of P and F 6D-lattices, these are the lattice node (0, 0, 0, 0, 0, 0) and the body-center of type (1, 1, 1, 1, 1, 1) / 2 that decomposes in four orbits in $\mathbf{E}_\parallel$, all of little group *m*35.

Using these two positions, we generate several important orbits as those given in Fig. 4. The best σ_0 is defined by the elementary triacontahedron, convex hull of the projection in $\mathbf{E}_\perp$ of the primitive unit cell, rescaled by τ^{-2} and truncated along the 5f-directions as introduced long ago by Henley [7, 16]. We designate it for short as the *Henley Triacontahedron* and note it T_H in Fig. 4 (on top left).

Close examination of the large ASs noted from 1 to 9 in Fig. 4 shows that the T_H of the orbits 1 to 4 around the node, and those of the orbits 5 and 6 around the bc, are remarkably optimized: the T_H are perfectly connected together by either the 2f- or 5f-directions with no overlaps. Moreover, the ASs 1 to 4 on the node and 5 and 6 on the bc fit perfectly, here too with no overlaps between the T_H. These basic ASs in $\mathbf{E}_\perp$ generate the following cluster orbits in $\mathbf{E}_\parallel$ (see [17, 18]):

T_1: center of the cluster localized at (0, 0, 0, 0, 0, 0);

T_2: icosahedron of radius[3] $\sqrt{2+\tau}$ (1.902) localized at (0, 0, 0, 0, 0, 1) and equivalents;

T_3: icosidodecahedron of radius 2 localized at (0, 0, 0, 0, 1, 1) and equivalents;

T_4: dodecahedron of radius $\sqrt{6-3\tau}$ (1.07) localized at (0, 0, 0, 1, 1, 1) and equivalents;

T_5: dodecahedron of radius $\sqrt{3}$ (1.732) localized at $(1, 1, 1, \bar{1}, \bar{1}, \bar{1})/2$ and equivalents;

T_6: icosahedron of radius $\sqrt{3-\tau}$ (1.1756) localized at $(\bar{1}, 1, 1, 1, 1, \bar{1})/2$ and equivalents.

This set is the simplest set of atomic orbits built from the node and bc sites of the 6D-lattice. It can be resumed in a first shell generated by T_4 plus T_6 forming an inner triacontahedron, a second shell generated by T_2 plus T_5 forming a second triacontahedron τ times larger, and finally a third shell generated by T_3 that forms a icosidodecahedron.

The three remaining ASs noted 7 to 9, have T_H that intersect each others, and therefore, their corresponding clusters share common atoms. These ASs generate:

T_7: dodecahedron of radius $\sqrt{3+3\tau}$ (2.802) localized at (1, 1, 1, 1, 1, 1)/2 and equivalents;

T_8: icosahedron of radius $\sqrt{3+4\tau}$ (3.078) localized at $(1, 1, 1, 1, 1, \bar{1})/2$ and equivalents;

T_9: icosidodecahedron of radius 2τ (3.236) localized at (1, 1, 0, 0, 0, 0) and equivalents;

T_7 and T_8 generate the third triacontahedron τ times larger than (T_2, T_5) and that links the inner atomic clusters.

All together, as already described in [17], the atomic orbits generated by the highest symmetry special points only are three concentric triacontahedra of increasing size by ratio of τ and two icosidodecahedra of sizes in the same ratio. These are shown in Fig. 4.

The other special points of *Pm*35 and *Fm*35 have lower symmetry and are listed in Table 2. Among them, are the mid-edge locations (1, 0, 0, 0, 0, 0) / 2 of symmetry $\bar{5}m$ and the mid-facet locations (1, 1, 0, 0, 0, 0) / 2 of symmetry *mmm* that both will play an important role for the Mackay clusters 6D descriptions as will be made clear in the next section. Their corresponding ASs, constructed using formula 4, are shown in Fig. 5. These ASs are made of 2 adjacent T_H, connected along a fivefold for the mid-edge position and along the twofold for the mid-facet position with little groups, respectively $\bar{5}m$ and *mmm*. Observe that the small size of the present AS is compensated by the multiplicity of the site. For example, for a *P*-

[3] All distances are given in $A/\sqrt{2(2+\tau)}$ where A is the 6D-lattice parameter.

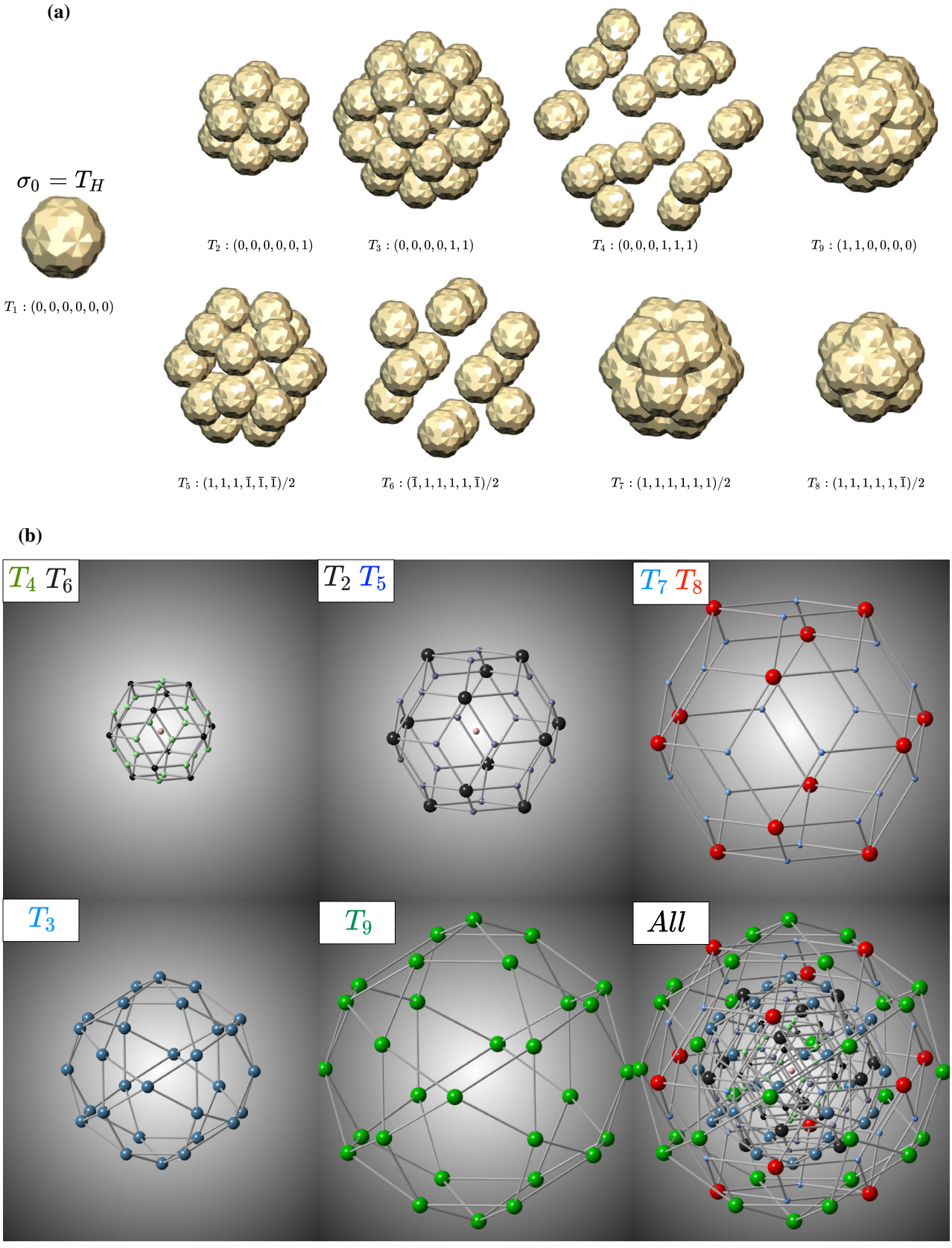

Fig. 4 *Top* optimal atomic surfaces associated with the main orbits generated by the nodes and body-centers for *P* and *F* 6D-lattices using the Henley triacontahedron T_{H} as σ_0. *Bottom* the corresponding atomic clusters

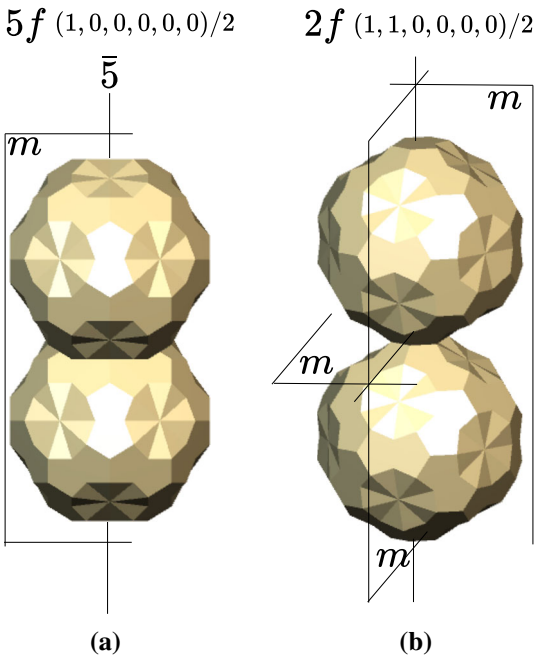

Fig. 5 Typical ASs for secondary special points for a *P*-type 6D lattice, **a** the mid-edge AS, say *ME*, along 5f of little group $\bar{5}m$ and **b** the mid-facet AS, say *MF*, along 2f of little group *mmm* (see Table 2)

type 6D lattice, the mid-edge AS has a volume of 2 in T_H units, but the position has multiplicity $|m35|/|\bar{5}m| = 120/20 = 6$ so that the total volume is $6 \times 2 = 12$ equal to the volumes of T_1 and T_6; the same applies for the mid-facet position with an AS of volume 2 but has multiplicity $|m35|/|mmm| = 120/8 = 15$ and thus corresponds to a total volume of $15 \times 2 = 30$ equal to the volume of T_3.

The Mackay clusters

The easiest way of generating Mackay-type clusters in the 6D approach is to select the ASs corresponding to high-symmetry locations leading to the simplest Mackay-type cluster $M_1 = \{T_1, T_3, T_2, T_6\}$, as seen on the left of Fig. 6 and made of an inner small icosahedron of radius $\sqrt{3-\tau}$, a large icosahedron of radius $\sqrt{2+\tau}$ and an icosidodecahedron of radius 2. This cluster differs from the original Mackay cluster in two ways:

- the size ratio of the two icosahedra is $\sqrt{(3-\tau)/(2+\tau)} = \tau - 1$ (≈ 0.618) instead of 1 / 2;
- the size ratio of the icosidodecahedron with respect to the large icosahedron is $2/\sqrt{2+\tau}$ (≈ 1.05) instead of $\tau/\sqrt{2+\tau}$ (≈ 0.85).

These two discrepancies can easily be eliminated as shown in Figs. 7 and 8:

- to correct the inner icosahedron, we remove T_6 located on the high-symmetry special point *bc* and replace it by *ME*, the AS located at the mid-edge (Fig. 5a); as already noted, this makes nothing else but shrinking the radius of the icosahedron from $\tau - 1$ to 1 / 2;
- to correct the icosidodecahedron, we remove T_3 located at the high-symmetry special point *n* and replace it by *MF*, the AS located at the mid-facet (Fig. 5b) that shrinks the radius of the icosidodecahedron from 2 to τ.

Finally, performing the two changes together leads to the 6D definition of the exact original Mackay cluster on the right in Fig. 6 $M_2 = \{T_1, ME, T_2, MF\}$ where *ME* and *MF* are the ASs, respectively, (a) and (b) of Fig. 5.

Mackay clusters in approximants and icosahedral phases

To compare these geometric considerations with actual structures showing Mackay-type clusters, we choose the 1/1 cubic approximants in the (Sc,Ru), (Al,Fe,Si), (Al,Mn,Si) and (Al,Fe,Si) alloys. We take the radius of the large icosahedron, R_{ico} as the reference for measuring the quality of the approximant (Fig. 9):

$$R^0_{ico} = A_6 \tau^{-1}/\sqrt{2} \quad \text{where} \quad A_6 = a\sqrt{(7-4\tau)/2} \approx 0.5137\ a \tag{5}$$

for a perfect 1/1 cubic approximant of parameter *a*.

The values of the various radii are given in Table 3. We observe that the experimentally determined radii of the shells of the clusters are between the two models; the radius R_{ico} of the large icosahedron deduced from the length of the cubic lattice parameter is in quite good agreement of what is expected from the models: These three structures can indeed be qualified as good approximants of the icosahedral phase. The radius r_{ico} of the small icosahedron is a bit larger that the one of the Mackay model for α-AlMnSi and α-AlFeSi, but significantly closer to the one of the ideal $\mathbb{Z}$-model for (Sc,Ru). Finally, in all three cases, the size of the icosidodecahedron is much closer to the value of the ideal $\mathbb{Z}$-model than from the Mackay model. This is not surprising because this second shell of the cluster is occupied by two different types of atoms, one for the large icosahedron and the other for the icosidodecahedron. A best compromise to relax short distances along the edge of the elementary tetrahedra is to increase the size of the icosidodecahedron up to its natural $\mathbb{Z}$-module value. This is clearly the most evident effect of the present comparison: The $\mathbb{Z}$-model is very efficient for generating an initial set of atomic positions in Mackay clusters, then relaxations occur that optimize the

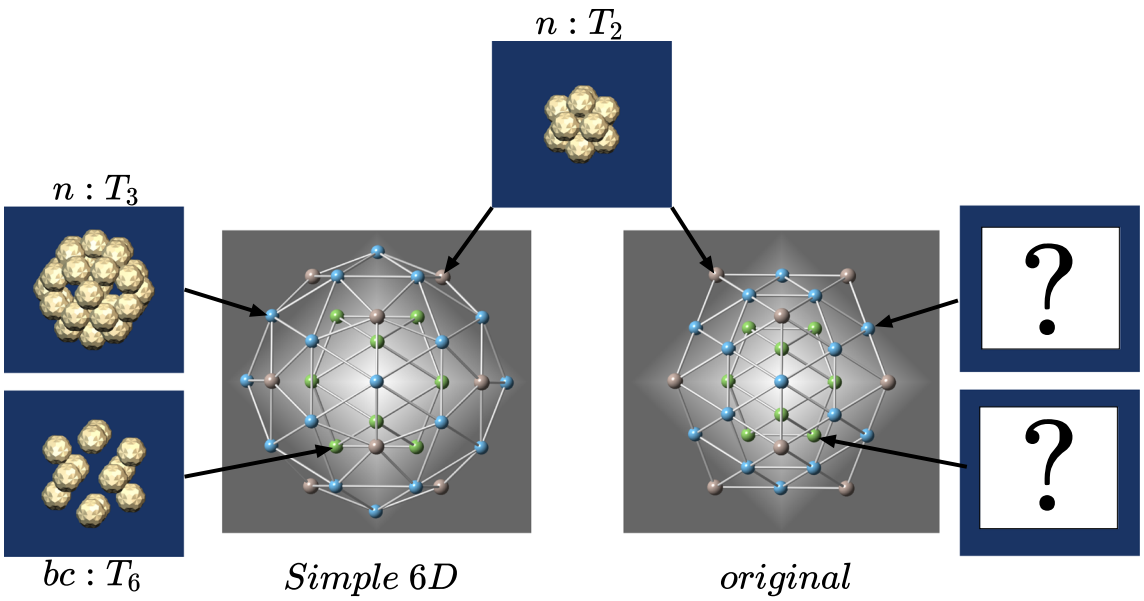

Fig. 6 Simplest Mackay-type cluster issued from 6D is generated using T_1, T_2, T_3 and T_6. It differs significantly of the original Mackay in the sizes of the inner icosahedron and of the icosidodecahedron

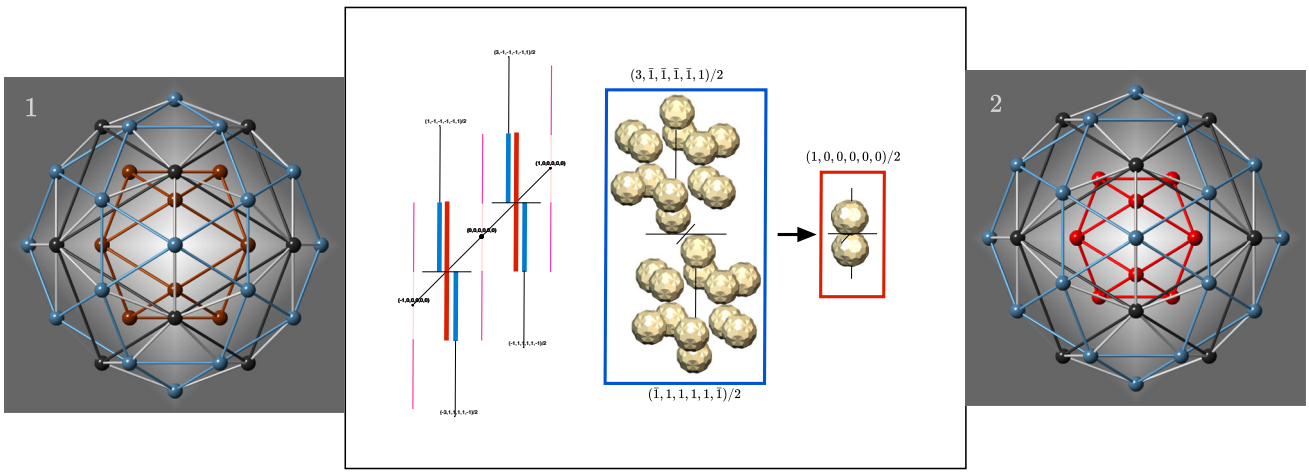

Fig. 7 Correcting the size of the inner icosahedron consists in moving two T_0's subAS issued from $(3,\bar{1},\bar{1},\bar{1},\bar{1},1)/2$ and $(\bar{1},1,1,1,1,\bar{1})/2$ at the level of (1, 0, 0, 0, 0, 0)/2, thus leading on removing T_6 at *bc* and replacing it by *ME* at mid-edge

interatomic distances and leave to the actual equilibrium atomic positions that are between the two models.

Beyond Mackay clusters

The two first shells of the so-called *Bergman* cluster originally discovered by Bergman et al. [19] in $(AlZn)_{49}Mg_{32}$ are made of:

- a center (possibly empty);
- a small internal icosahedron;
- a large icosahedron (twice larger);
- an large dodecahedron forming a triacontahedron with the large icosahedron.

This cluster is very similar to the original Mackay except that the second shell corresponding to the large triacontahedron is the large icosahedron completed by atoms along the ternary axes (dodecahedron) instead of the binary axes (icosidodecahedron). This cluster of 44 (+1) atoms is slightly lighter than the Mackay one.

The lifting of the Bergman in the 6D space is very simple and similar to the one previously performed for the original Mackay. The small inner icosahedron is generated by locating *ME* ASs at the mid-edge. The large

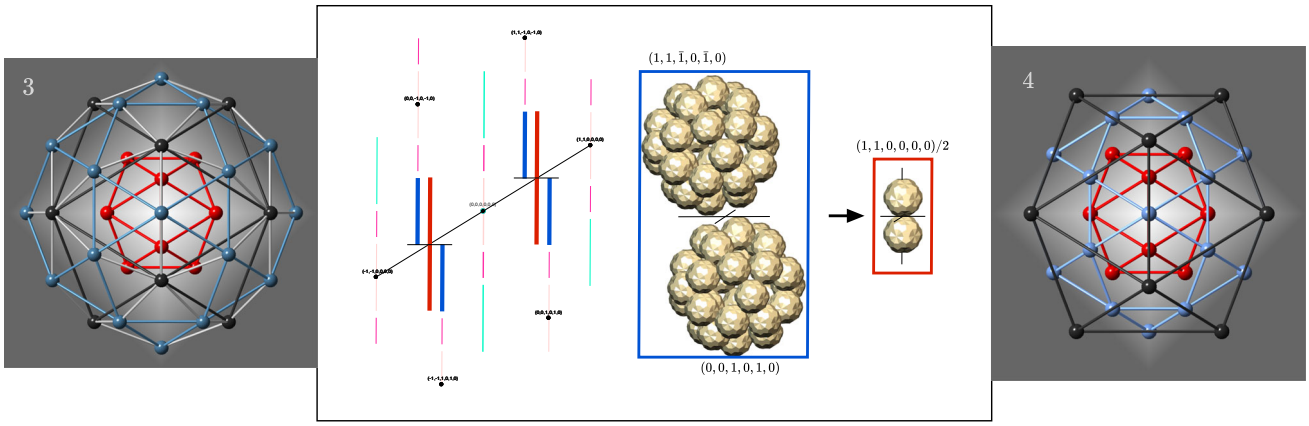

Fig. 8 Correcting the size of the outer icosidodecahedron consists in moving two T_0's subAS issued from $(1, 1, \bar{1}, 0, \bar{1}, 0)$ and (0, 0, 1, 0, 1, 0) at the level of (1, 1, 0, 0, 0, 0) / 2, thus leading on removing T_3 at *n* and replacing it by *MF* at the mid-facet

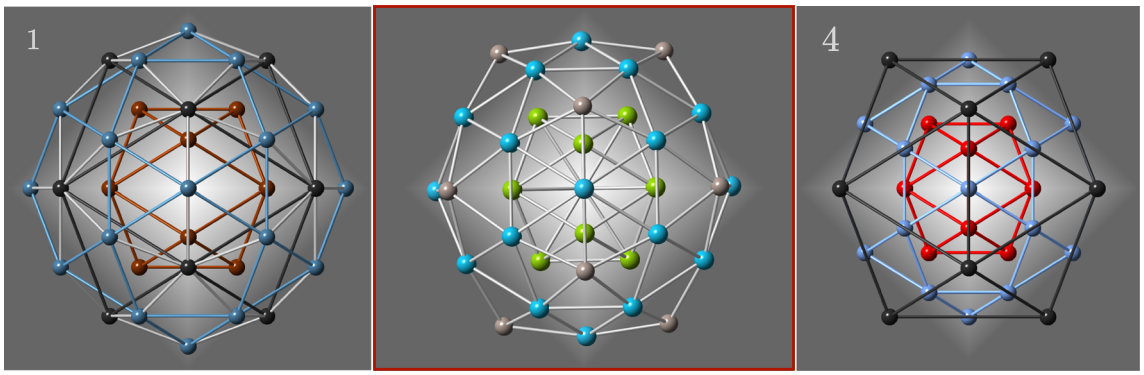

Fig. 9 Mackay clusters of the (Sc, Ru) 1/1 cubic approximant phase drawn in the middle are almost exactly between the two ideal models, the 6D natural cluster on the *left* and the original Mackay cluster on the *right* (see Table 3)

Table 3 Radii of the basic shells of the Mackay cluster for the original Mackay ideal model, the simple $\mathbb{Z}$ model, and for three Mackay clusters as experimentally determined in (Sc,Ru), α-AlMnSi and α-AlFeSi structures

	Original Mackay	Natural 6D	$Sc_{57}Ru_{13}$ *bc*	(A = 1.4394 nm) *n*	α-AlMnSi *bc*	(A = 1.268 nm) *n*	α-AlFeSi *bc*	(A = 1.231 nm) *n*
r_{ico}	0.5	0.618	0.570	0.574	0.534	0.527	0.543	0.534
R_{ico}	1.0	1.0	1.074	1.074	1.027	1.057	1.045	1.015
$R_{icosi(6)}$	0.85	1.05	0.995	1.031	1.069	1.00	1.059	1.059
$R_{icosi(24)}$	0.85	1.05	0.995	1.018	1.029	1.025	1.044	1.046

icosahedron is as usual generated by T_2 at the node and the large dodecahedron is generated by T_5 at the bc (see the T_2T_5 subfigure in Fig. 4). Thus, as often quoted in the $Im\bar{3}$ cubic phase $(AlZn)_{49}Mg_{32}$ determined by Bergman et al. is an excellent 1/1 cubic approximant of an hypothetical icosahedral phase of 6D-lattice parameter $A_6 = 0.7274$ nm.

Numerous new icosahedral quasicrystals have atomic structures based on the so-called Tsai cluster that has been discovered in the *i*-$Cd_{5.7}Yb$ = *i*-$Cd_{85}Yb_{15}$ binary alloy (see for instance [18, 20–22]). Taking a 6D-lattice parameter of $A = 0.80$ nm, we can describe the Tsai cluster as:

- an empty center;
- a small dynamically distorted inner tetrahedron;
- an inner Cd dodecahedron also dynamically distorted of average radius 0.46 nm;
- a basic Yb icosahedron of radius 0.57 nm;
- a Cd icosidodecahedron of radius 0.65 nm;

Table 4 Comparison of radii expe/theo in the Tsai-type cluster as observed in *i*-YbCd. The error is estimated by $\delta = (r_{theo} - r_{expe})/r_{theo}$. Even for the basic reference icosahedron, the actual orbits of the Tsai shells show strong deviations from their corresponding ideal images on the 6D lattice

YbCd	Exp	Theo	Error δ (%)
Small dodecahedron	0.46	0.52	−12.0
Base icosahedron	0.56	0.569	−1.5
Icosidodecahedron	0.65	0.6	+8
Triacontahedron (along 2-f)	0.78	0.746	+4

- a large triacontahedron of radius 0.78 nm along the twofold directions, with atoms at the middle of the edges.

Contrary to the Mackay case, the corresponding 6D-lattice nodes are definitely not obvious to be found.

First, there is no 6D-orbit that would generate the small tetrahedron owning the fact that none of the standard cell decompositions of ASs generating dodecahedra can give the ratio of 4/20. The simplest artifact that can be used to simulate this tetrahedron is to introduce the inner dodecahedron generated by T_4 with an statistical occupation factor of 4 / 20.

The situation is slightly better for the small Cd dodecahedron of radius of 0.46 nm which can be approximated by the AS T_5 localized in $(\bar{1}, 1, 1, 1, 1, 1)/2$ corresponding to a radius of 0.515 nm instead of the expected 0.46 nm.

The large Yb icosahedron is the reference orbit out of which the 6D-lattice parameter A has been calculated: the AS T_2 localized at (1, 0, 0, 0, 0).

The Cd icosidodecahedron can be approximately generated by T_3 localized at $(0, 1, 0, 0, \bar{1}, 0)$ with a radius of $0.7435\ A = 0.595$ nm instead of 0.65.

Finally, the large triacontahedron can be generated by T_7 at (1, 1, 1, 1, 1, 1) / 2 and T_8 located at $(1, 1, 1, 1, 1, \bar{1})/2$ with atoms at 0.833 nm along the 3-f, 9.15 nm along the 5-f and 0.828 nm along the 2-f instead of the 0.78 nm expected. The atoms at the middle of the edges of this triacontahedron are generated by a original new AS located at (1, 1, 1, 1, 1, 0) / 2.

These results are summarized in Table 4 that shows quite important deviations between the actually observed radii of the various orbits and their theoretical values issued from the 6D special points description.

Conclusion

We have shown here how the lifting in 6D space of the original Mackay and Bergman clusters is simple and natural with very little distortion between theoretical and experimentally determined atomic positions. This lifting is far from being as simple for the Tsai clusters that show an inner shell that is unexplained by the 6D scheme and is finally constructed using large displacements in the physical space from the theoretical positions of the $\mathbb{Z}$-module. This is by no mean in contradiction with the 6D approach where it is always possible to shift atoms in the parallel space consistently with the local internal symmetry; it is, however, clearly the sign that, in that case, the ideal 6D special points approach—that is still the most efficient tool for building ideal basic structures—does require large local relaxations to conform the ideal model to the experimental diffraction data.

Acknowledgments This work has been made possible by the financial support of ANR-13-BS04-0005-01 METADIS that is warmly acknowledged.

References

1. Shechtman D, Blech I, Gratias D, Cahn JW (1984) Phys Rev Lett 53:1951
2. Mackay AL (1981) Kristallographiya (Sov Phys Crystallogr) 26(5):910–919
3. Mackay AL (1982) Phys A 114:609
4. Mackay AL (1962) Acta crystallogr 15:916
5. Guyot P, Audier M (1985) Philos Mag B 52(1):L15
6. Audier M, Guyot P (1986) Philos Mag B 53:L43
7. Henley CL (1985) J Non-Cryst Solids 75:91
8. Elser V, Henley CL (1985) Phys Rev Lett 55:2883
9. Gratias D, Puyraimond F, Quiquandon M, Katz A (2000) Phys Rev B 63:024202
10. de Bruijn NG (1981) Nederl Akad Wetensch Proceedings Ser A 84:38–66
11. de Bruijn NG (1987) In: Steinhardt PJ, Ostlund S (eds) The Physics of Quasicrystals. World Scientific Publishing Company, Singapore, pp 673–700
12. Duneau M, Katz A (1985) Phys Rev Lett 54:2688
13. Elser V (1985) Phys Rev B 32:4892
14. Kalugin PA, Kitaev AY, Levitov LC (1985) J Phys Lett 46:L601
15. Janssen T (1986) Acta Crystallogr A 42:261–271
16. Henley CL (1985) J Non-Cryst Solids 75:91; ibid Phys Rev B 34:797–816
17. Quiquandon M, Gratias D (2014) Comptes Rendus Phys 15(1):18
18. Takakura H, Gomez CP, Yamamoto A, de Boissieu M, Tsai AP (2007) Nat Mater 6:58
19. Bergman G, Waugh JLT, Pauling L (1957) Acta Crystallogr 10:254–259
20. Tsai AP, Guo JQ, Abe E, Takakura H, Sato TJ (2000) Nature 408:537–538
21. Guo JQ, Abe E, Tsai AP (2000) Phys Rev B 62:R14605–R14608
22. Yamamoto A, Takakura H, Tsai AP (2003) Phys Rev B 68:094201